EFFECT OF NEWTONIAN AND NON-NEWTONIAN FLOW IN SUBJECT SPECIFIC CAROTID ARTERY

NITESH KUMAR[1], S. M. ABDUL KHADER[1,*],
RAGHUVIR B. PAI[1], PANICOS KYRIACOU[2], SANOWAR KHAN[2],
K. PRAKASHINI[3], D. SRIKANTH RAO[1]

[1]Department of Mechanical and Manufacturing Engineering, Manipal Institute of Technology, Manipal Academy of Higher Education, Manipal, 576104, Karnataka, India
[2]School of Mathematics, Computer Science and Engineering, Department of Electrical and Electronic Engineering, City, University of London, London, UK
[3]Department of Radio-diagnosis, Kasturba Medical College and Hospital, Manipal Academy of Higher Education, Manipal, 576104, Karnataka, India
*Corresponding Author: smak.quadri@gmail.com

Abstract

Advances in the numerical simulation techniques has immensely helped in the demonstrating the importance of blood flow through elastic arteries and evaluating the disease progression and flow dynamics of cardiovascular diseases such as atherosclerosis. The present work deals with a case study of a patient diagnosed with partial narrowing of entire cervical segment of Internal Carotid Artery (ICA), while Common Carotid Artery (CCA) and External Carotid Artery (ECA) appears to be normal. Subject specific 3D carotid bifurcation CAD model is generated based on CT-angio scan data using MIMICS-14.0 and numerical analysis is performed using Computational Fluid Dynamics (CFD) in ANSYS-CFX-14.0. Pulsatile blood flow through the subject-specific artery is investigated to study the influence of rheology on the haemodynamics in the blood flow. The simulation results obtained through Carreau-Yasuda and Newtonian models are investigated. Flow behaviour observed during peak systole exhibits significant difference in the spatial parameters between both the Newtonian and non-Newtonians models. The comparison of local shear stress magnitude in CCA, ICA and ECA demonstrates that WSS is highly influenced by the shear thinning property of blood. This variation is also observed artery branches with reduced lumen diameter, lumen narrowing due to stenosis and in the bifurcation zone.

Keywords: ANSYS CFX , Carotid bifurcation artery, Newtonian and Carreau - Yasuda model, Wall shear stress.

1. Introduction

Numerical simulation has advanced in recent years and significantly contributed in examining the cardiovascular diseases. These studies shall be useful in understanding the mechanics of normal and diseased arteries by clinicians/researchers [1]. Numerical methods have exhibited remarkable progress in investigating the blood flow as experimental method have their limitation in measuring haemodynamic parameters. The flow behaviour in stenosed artery is depicted with elevated stresses and high resistance to flow when compared with the normal and healthy artery. Atherosclerosis in carotid system is the root cause of about 80% of strokes [2]. Deposition of soft structure plaques forms arbitrary and irregular areas inside the arteries. At this deposition site, the platelets fill-up the cracked irregular areas resulting in forming blood clot in the artery or its branches causing atherosclerosis. The bifurcation zone and the inner curvature of the vasculature is favourable site for atherosclerotic plaque deposition and also more prone to localized regions of low WSS [2, 3]. On contrary, high WSS is protective towards atherosclerosis formation while the region of low WSS is prone to atherosclerosis. Hence, the initiation of thickening of arterial wall begins at the region of low WSS [3-7]. Haemodynamic parameters such as flow velocity, WSS are evaluated based on CFD simulation techniques based on accurate boundary condition, computational time and clinical expertise. Clinically, flow velocity certainly be obtained by phase contrast MRI (PC-MRI) technique. It is also observed that PC-MRI technique underestimates the velocity and WSS magnitude due to lack of spatial resolutions [8]. However, MRI based WSS will result in similar pattern as obtained through CFD simulation in investigating the pulsatile flow in carotid bifurcation system. This is achieved through combining the data from MR imaging with CFD modelling [9, 10]. It was observed that MR measurements were inadequate to portray the secondary flow pattern and hence a combination of MR and CFD was more useful to obtain reliable flow velocity details. Gijsen et al. [11] also demonstrated the local hemodynamic parameters are governed by both pulsatile pressure, bifurcation geometry along with the properties of the arterial wall and blood rheology. Computational methods also provided an alternative for *in-vivo* measurement techniques like MRI to obtain accurate haemodynamics in vasculature which help demonstrate the risks of plaque rupture.

Adopting appropriate boundary conditions effects the solutions and influence the haemodynamics in an image based simulation models. It is recommended in several studies to adopt boundary conditions closer to the realistic constraint to evaluate the prognosis of outcomes and relate an alternate therapeutic interventions and role of local fluid dynamics and other biomechanical factors in vascular diseases [12]. Ladak et al. [13] reported that realistic human vasculature requires accurate techniques for investigation of haemodynamics. Rapid extracting technique was adopted to generate the arterial geometry from MR images and simulation methods to study the haemodynamics of the vasculature. It was found that, carotid artery stenosis severity was the major indicator of risk of stroke. However, it was observed that individuals suffered from stroke having medium or mild stenosis when compared with patients who were safe from stroke even with severe carotid stenosis [14, 15]. Some of the haemodynamic factors along with severity of stenosis plays a major role in predicting the risk of stroke as reported in Stroud et al. [16]. They demonstrated the accurate indications of vulnerable plaques as observed from the study of effect on the flow patterns through the computational

simulations. Flow separation zones at the post stenotic regions were complex depending on the degree of stenosis and oscillations of WSS at the downstream of stenosis resulted in the low WSS regions [17,18].

As observed in previous studies, blood flow in the carotid system was modelled as Newtonian fluid and shear thinning characteristics were ignored, arguing that the shear rate in large arteries are high and the blood viscosity was considered equal to high shear rate viscosity limit [19-22]. In addition to this assumption, geometry of the anatomically realistic arteries were simplified and idealistic computational models were considered to simulate blood flow [23, 24]. However, when idealistic and anatomically realistic models of carotid artery compared, it was observed that the idealized model masked some of the key observations when compared with realistic models [25]. Patient care can be improved with better treatments by combining computational simulation with the individual patient specific data in order to enhance the knowledge of vascular haemodynamic details and study the clinically relevant blood flow problems.

Chan et al. [26] studied that blood is a shear thinning fluid and demonstrated that the general Newtonian model will not capture the haemodynamics at critical locations. This observation was supported by another study in abdominal aortic bifurcation in patient specific cases which shows that non-Newtonian model is able to capture this influence on velocity distribution and WSS [27]. Influence of non-Newtonian flow phenomenon in a carotid bifurcation system was studied by incorporating the shear thinning behaviour by using Carreau-Yasuda Model [28]. Non-Newtonian models are investigated in a stenosed elastic artery using the Carreau and the Power-law to determine the velocity, WSS and arterial wall displacement [29]. In another study, Carreau-Yasuda and Yeleswarapu models were mathematically modelled to study the flow inside a stenosed elastic artery and compared the WSS and oscillatory shear index (OSI) values with the Newtonian model [30]. Khairuzzaman et al. [31] carried out fundamental study on effect of non-Newtonian flow model in idealized carotid artery using cross- model and observed that this model was able to capture the WSS in more precise manner than Newtonian model. Further, blood flow in a coronary arterial bypass graft was investigated using Carreau-Yasuda model to evaluate the haemodynamic parameters and compared with the Newtonian model [32].

Among various models available to study the non-Newtonian flow such as Carreau-Yasuda, Power law, Carreau and Casson models, Carreau-Yasuda model is found to provide better and more accurate estimation of flow velocity especially at the critical site such as stenosis and geometric curvature. Significant differences was observed when compared with the Newtonian study and it was found that non-Newtonian properties of blood is an essential factor in haemodynamics and plays a very vital role in vascular biology [27-30]. Non-Newtonian assumption has also demonstrated the close agreement with clinical observation of low velocity zones and clotted-off regions in contrast to Newtonian studies [33]. Local viscosity model was proposed to capture high precision presentation of blood viscosity changes especially in bifurcation region and to observed that high viscosity zones substantially influenced the size of flow recirculation zone [15].

Several numerical studies are carried out to compare Newtonian and non-Newtonian models under steady and pulsatile flow conditions to measure flow patterns and critical shear stress regions [34-36]. An attempt is made in the present

study to carry out fundamental investigation to observe the shear thinning characteristics and significant variation among Newtonian and non-Newtonian models. Non-Newtonian study shall be carried out using Carreau-Yasuda model. This basic study shall be useful to carry out detailed observation of haemodynamics in critical regions such as stenosis and bifurcation zone. Hence, in the present study, subject-specific carotid bifurcation of partial narrowing of ICA is investigated and 3D geometric model is reconstructed using MIMICS and modelled in CATIA. Further, numerical simulation is carried out in ANSYS CFX to study the effect of non-Newtonian blood viscosity on the distribution of velocity, WSS and shear strain rate under pulsatile flow conditions. The shear thinning property of blood is also considered by using Carreau-Yasuda blood viscosity model and a detailed comparison between Newtonian and non-Newtonian model is presented.

2.Methodology

2.1. Theory

Numerical simulation of blood flow is governed by Navier Stokes equation and flow domain is solved by adopting control volume method wherein, the mass and momentum conserved for incompressible fluid is given by [37-39]

$$\nabla . \upsilon = 0 \tag{1}$$

$$\rho\left(\frac{\partial v}{\partial t} + v\nabla v\right) = \nabla P + \nabla \tau \tag{2}$$

Blood viscosity is calculated through constitutive equations. Different constitutive equations are proposed to model the flow of blood, but the simplest of them all is the Newtonian model, which assumes the viscosity as constant. For this model, the density of the fluid domain is 1050 kg/m^3, and dynamic viscosity is 0.004 N-sec/m^2 [39, 40]. Recently, many researchers have suggested different blood viscosity models incorporating the shear dependence of blood flow dynamics. Most commonly used non - Newtonian blood viscosity models are power law, Casson, and Carreau Yasuda models [30, 32]. The power law is expressed as [33].

$$\boldsymbol{\mu = k\dot{\gamma}^{n-1}} \tag{3}$$

Power law model is the quite simple and it is used to represent the non-Newtonian behaviour of the fluid. However, this models has a range from zero to infinite shear rate and only the values in the accurate range shall be able to estimate the non-Newtonian behaviour. Power law index is usually selected such that the model replicates the shear thinning behaviour in hemodynamic simulations [34]. The Casson model takes into account both the shear thinning behaviour and the yield stress of blood. However it is the Carreau Yasuda model which better fits the shear rate relationship and the experimental data [35, 36].

$$\frac{\boldsymbol{\mu-\mu_\infty}}{\boldsymbol{\mu_0-\mu}} = \boldsymbol{(1 + (\lambda\dot{\gamma})^a)^{(n-1)/a}} \tag{4}$$

This model is the simplest one used to represent the non-Newtonian behavior of the fluid. However, it has a range from zero to infinite shear rate and only the values in realistic range will approximate the non-Newtonian behavior. Also, the power law index is usually selected so that the model replicates the shear thinning behavior in hemodynamic simulations [34]. The Casson model takes into account

both the shear thinning behaviour and the yield stress of blood. However, it is the Carreau - Yasuda model which better fits the shear rate relationship and the experimental data [35, 40].

2.2. Modelling and analysis

In the present study, numerical simulation is carried out on a subject specific carotid bifurcation artery. This case study refers to a 75 year old male patient who is diagnosed with a right cerebral infarction (stroke). The left carotid system was normal, while the right CCA and ECA appears to be normal with partial narrowing (stenosis) of the complete visualized cervical portion of ICA. The percentage of area reduction is chosen at different locations in ICA and the average narrowing is approximately 60%. The right carotid bifurcation system is highlighted in the three different views as shown in the Fig. 1. The encircled area highlights the location of carotid bifurcation on the right carotid system in addition to the 3D geometric model generated in MIMICS. Since left carotid system is normal with no sites of plaque formation as observed in the CT angio scans and hence it is not considered in the present numerical simulation study.

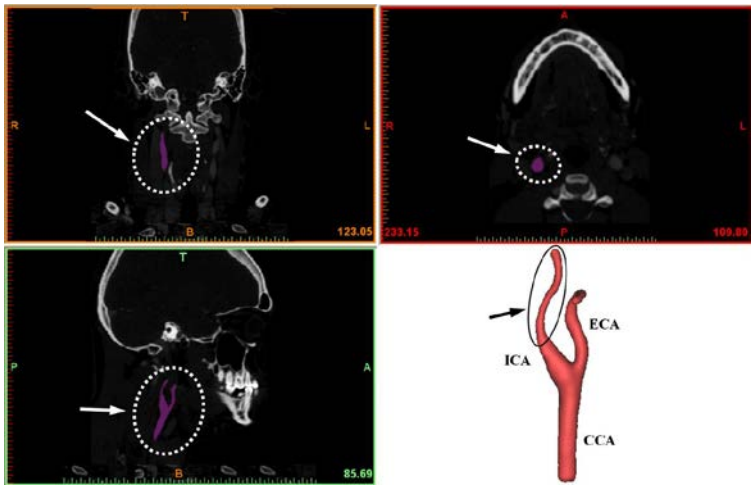

Fig. 1. Different views of CT scan of carotid bifurcation: Partially stenosed ECA at bifurcation tip.

3D geometric model is generated using MIMICS -14 based on CT angio data and surface smoothening and refining and refined is done in CATIAV5R20.0, versatile geometric modelling software. Further, numerical model is meshed with hexahedral elements using ICEM-CFD in ANSYS 14.0. 3D unsteady Navier Stokes equations were solved by implementing a finite volume scheme using ANSYS CFX (ANSYS Inc., Canonsburg, PA). Grid independency test is carried out for carotid bifurcation as accuracy of numerical results primarily depends on quality and quantity of the mesh. It also helps to resolve the velocity vectors and effectively capture the haemodynamics at critical zones in carotid bifurcation taken up in the present study. As the Reynolds number is 443, a laminar flow model was used to simulate the steady flow in the carotid system with convergence criterion of 10^{-5}. Flow variables such as maximum velocity and average pressures are

monitored for different grid sizes as shown in the Fig. 2. Based on the grid independency check as shown in Fig. 2, 3D carotid system is meshed with 82500 hexahedral elements.

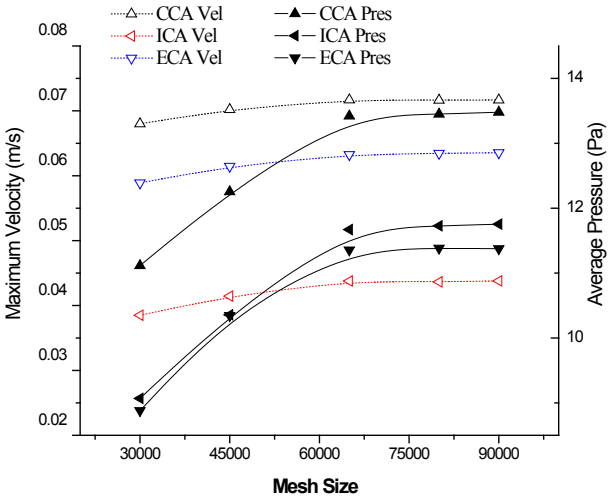

Fig. 2. Grid Independency study of carotid bifurcation.

A steady state analysis is performed for grid check to understand the haemodynamics at peak systole with inlet velocity of 0.93 m/s applied at inlet and at the outlets a constant pressure of 30 mmHg is applied [41, 42]. The walls of the carotid artery was considered as rigid with no slip condition. The variation of diameter along the CCA, ECA and ICA of carotid system is evaluated at the location where the diameter is minimum as observed from previous studies [38, 43]. However, even in large arteries where there is stenosis leading to reduction in diameter this assumption does not hold good since it masks the shear thinning character of blood [44, 45]. At the inlet, time dependent velocity wave form obtained by Ultrasound Doppler of a patient was prescribed as shown in the Fig. 3 which corresponds to the ultrasound waveform.

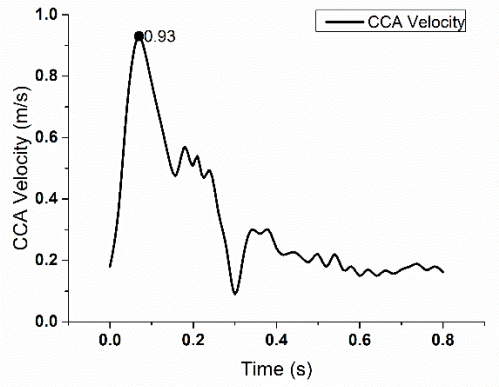

Fig. 3. Inlet Velocity waveform highlighting peak velocity at 0.072 s.

For outlets, an impedance method developed was implied by modelling the vascular system as a fractal network [36, 41]. In this method, the vessels beyond the imaging domain are approximated with the help of 1D flow approach [42]. The applied pressure waves on ICA and ECA are shown in Figs. 4 and 5. 3D meshed model with applied boundary conditions at the inlet and outlet is as shown in Fig. 6. Time step sensitivity is carried out for five different time steps (60, 120, 180, 240 and 300). Maximum velocity and average pressure is measured common section in CFD simulation. Based on the time sensitivity test, 180 time steps is adopted in the present CFD studies. Individual pulsatile cycle is considered for a time period of 0.8 s is discretized into 180 time steps to accurately capture the flow behaviour. The simulation results obtained is useful in providing comprehensive haemodynamic data to clinicians in diagnosing and evaluating clinical cases and thus indicating the potential of atherosclerotic progression and rupture.

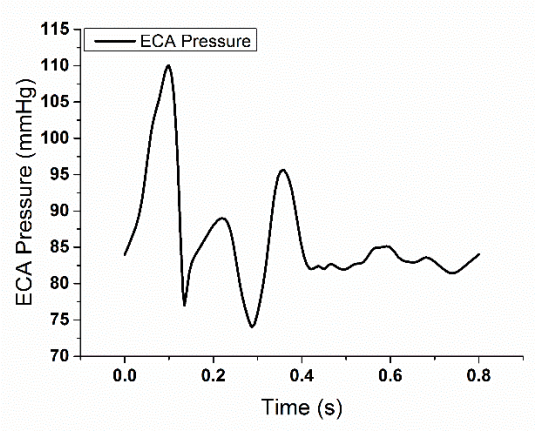

Fig. 4. Outlet pressure waveform at ECA outlet obtained by impedance boundary condition.

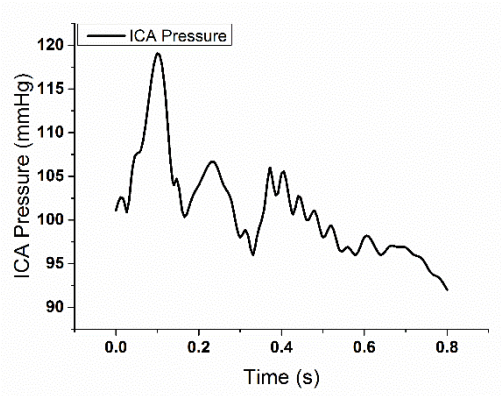

Fig. 5. Outlet pressure waveform at ICA obtained from impedance boundary conditions.

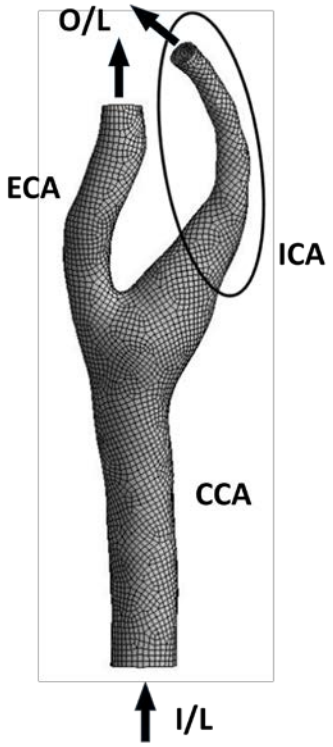

Fig. 6. Partially stenosed carotid bifurcation model

3. Results and Discussion

Haemodynamic changes in Newtonian and non-Newtonian flow models are investigated on important parameters such as WSS, velocity contours and pressure profiles. The maximum changes in the flow occur during peak systole are also compared. During grid study, the variation of diameter along the three branches of the carotid artery is calculated and a location where the diameter is minimum is located as indicated in Fig. 7. This observation is to support the assumption of blood as Newtonian fluid which is found to be valid in larger arteries due to higher shear rates.

Figure 7 shows the variation of diameter along the axis of CCA, ICA and ECA and the location where the diameter is minimum is highlighted. In this location WSS is captured along the circumference of the ICA and it can be seen in Fig. 8 which shows that the Newtonian model overestimates the WSS in critical location [40, 43, 46]. Similar overestimation of WSS at entire ICA is represented in the Fig. 9. Spatial variation of WSS contour along the CCA and ICA as highlighted and compared between Newtonian and non-Newtonian flow models as described in the Fig. 9 [25, 26, 40]. WSS increases significantly towards the cervical apex of ICA due to increased velocity at the stenosis site. High wall shear stress in an indicator of plaque rupture [45]. The is due to the assumption of constant viscosity by Newtonian model at every location, but as blood is a shear thinning fluid the viscosity is highly dependent on the geometry and the applied boundary conditions.

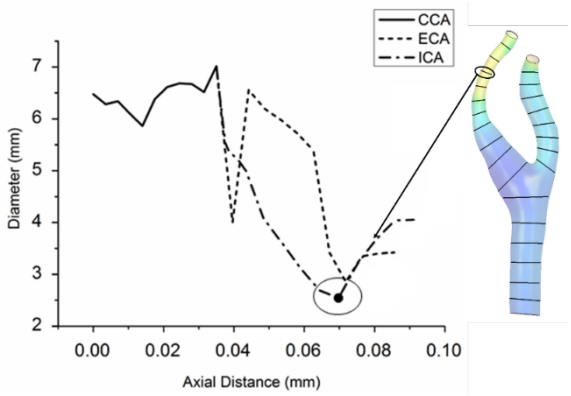

Fig. 7. Variation of diameter along CCA, ICA and ECA highlighting the location where the diameter is minimum.

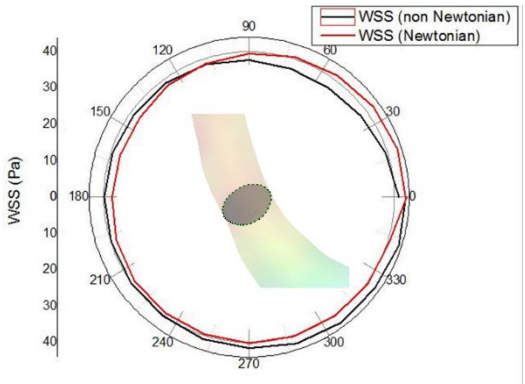

Fig. 8. Variation of WSS at the neck of the stenosis in ICA at peak systole showing the over estimation of WSS

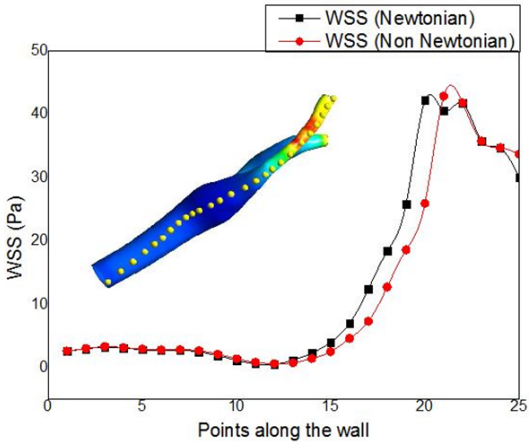

Fig. 9. Spatial variation of WSS along CCA and ICA.

Figure 10(a) represents the velocity contour, while Fig.10(b) shows the velocity streamlines during peak systole with increased velocity in entire ICA. Velocity contour also includes the planes at different intervals in CCA, ICA and ECA as highlighted in the Fig. 10(a). There is substantial increase in the flow velocity at the site of partially stenosed ICA of concentric nature. It is widely known that if the area reduction is less than 70%, the flow sharing does not change significantly.

The bifurcation zone especially at the carotid bulb oriented towards the ICA root clearly shows the intense flow separation zone and this is characterised by extending to longer region towards the downstream side of ICA [41].The maximum velocity value at peak systole is increased insignificantly in the non-Newtonian model. The high velocity regions at mid-diastole are reduced in the non-Newtonian model. The overall velocity vector patterns of the aorta for a non-Newtonian fluid model are similar to velocity vector patterns of a Newtonian fluid model.

Pulsatile flow analysis is carried out using inlet velocity waveform and outlet pressures. Haemodynamic parameters such as WSS, velocity and diameter is calculated along the axis of the carotid system during peak systole where the velocity is maximum [46]. The WSS distribution in carotid system is found to be slightly higher in CCA, drastically reduces at the bifurcation zone, and it increases again along the inner wall of ECA and distal end at ICA. Mild partial stenosis in ICA has influenced the highly disturbed WSS behaviour mainly at the bifurcation zone [37, 38]. The bifurcation region is also characterized by flow separation which is observed to be moderately intense causing significantly low WSS and covering larger area in CCA and ICA region.

The average WSS at the bifurcation was 5 Pa and the maximum WSS was found to be 42 Pa at the stenosis site. The WSS map revealed a large region of low WSS at the bifurcation zone and extended to the outer wall in the proximal end of the internal carotid artery, with the lowest value below 0.5 Pa. Further, there is significant rise in WSS, especially at the apex towards the inner wall of ECA, and it extends to maximum at stenosed region in right ICA [32, 47]. The highly disturbed flow at the bifurcation zone will significantly increase the vortex formation and it also influences the atherosclerotic damage to arterial wall. The shear stress has spread to quite larger area which is occupied by ICA and the bifurcation zone.

Figure 11 shows the variation of velocity, WSS and diameter of CCA during the peak systole and it demonstrates that there is no qualitative and significant quantitative difference between the Newtonian and Carreau-Yasuda blood viscosity models. However, there is slight increase in the value of WSS with Newtonian model at plane 4 in CCA when compared to Carreau-Yasuda model. It also depicts the flow recirculation and low WSS as can be seen clearly in the streamlines shown in Fig. 10(b). The average diameter throughout the length of the CCA is 6.5 mm. Any artery above 6mm in diameter is generally considered as large arteries and as observed from the plots that the shear rate is above 100 s^{-1}. Blood can be considered as Newtonian fluid for lumen diameter greater than 6mm and also for shear rates above 100 s^{-1}, however, when there is flow circulation or reverse flows Newtonian models does not give correct results [33, 46].

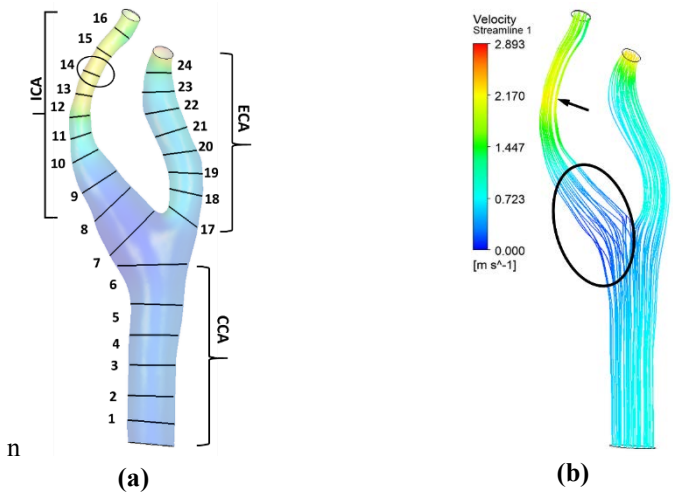

Fig. 10. (a) Velocity contour with details of plane considered during peak systole in Newtonian model and (b) Velocity streamlines during peak systole in non-Newtonian model.

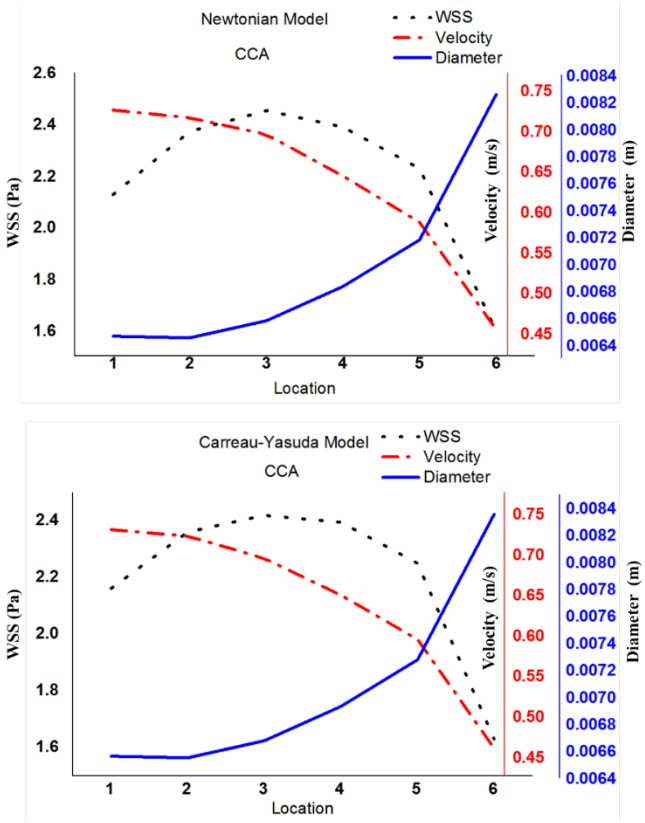

Fig. 11. Variation of WSS, velocity and diameter along the axis of CCA.

Similarly, even in the case of ECA there is no qualitative differences between the Newtonian and Carreau Yasuda model. However, there is small over estimation of WSS with Newtonian model compared to Carreau-Yasuda model as shown in Fig. 12. The average diameter of the ECA is 5 mm which can also be considered as large artery hence Newtonian model will give satisfactory estimation of the haemodynamics. The average diameter of ICA is 4mm. Fig. 13 explains that, the Newtonian model shows significantly high values of shear stress when compared to Carreau Yasuda model at the location where the diameter is around 2mm i.e., at the neck of the stenosis. This is the clear indicator of failure of Newtonian model to accurately predict the haemodynamics at low diameter regions [26, 27]. In other locations where the diameter is higher there is no much difference between the two models.

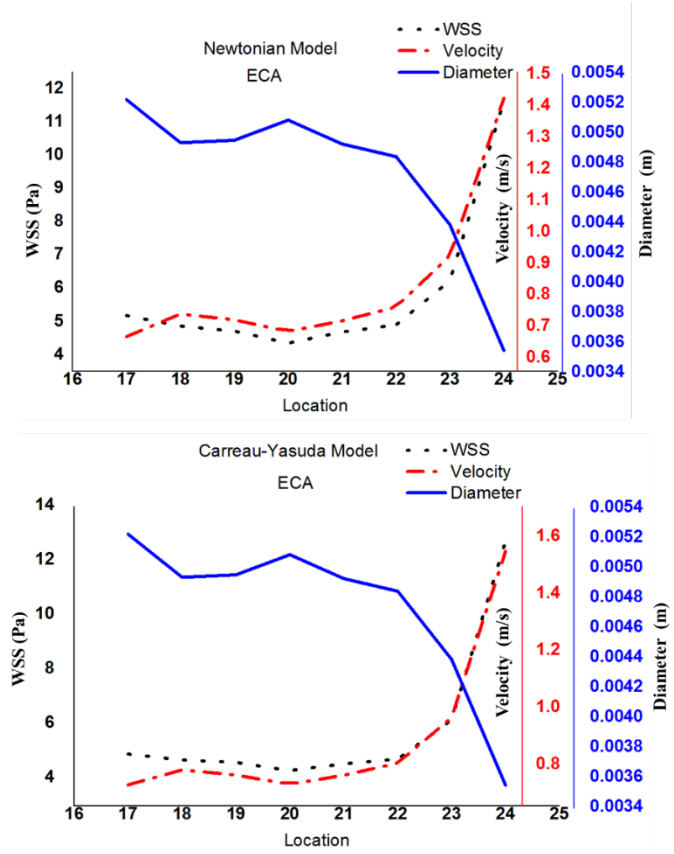

Fig. 12. Variation of WSS, velocity and diameter along the axis of ECA.

From the Fig. 12, it is evident that the velocity peaks at the site of stenosis. Also, Figs.11, 12 and 13 shows that velocity profiles of the Carreau Yasuda model has significant change when compared to the Newtonian model. For both these models, during the decelerated flow phase, a reversed flow region was found to be intense along the outer wall of the carotid bifurcation, more predominant in ICA (Fig. 10(b)). However, the reversed velocity from Carreau Yasuda model was lower than the Newtonian model. Low shear rate is more dominant as observed at the centre-

line of the artery, while high shear rate near the arterial wall in the non-Newtonian flow in comparison to Newtonian model [47]. However, the impact of non-Newtonian effects is not dominant on velocity profiles on these regions. Overall, there is general agreement of flow patterns for the both non-Newtonian and Newtonian model however the size and velocity of the flow recirculation zones are significantly affected by the non-Newtonian fluid model and should be considered. Newtonian model has overestimated the velocity magnitude as observed from velocity profiles at various planes during entire pulse cycle and neglecting the non-Newtonian rheology could lead to overestimation of haemodynamics stress in carotid artery bifurcation [45].

The distribution and location of WSS was similar and agreed for both the Carreau Yasuda model and the Newtonian model. The time-WSS plots showed similar shape with that of the velocity, and the curves pattern of both these models are superposed with each other at most of the locations. However, there is a slight delay in Newtonian model especially at the centre of CCA, root of ECA and at stenosis site in ICA zones in comparison to non-Newtonian model. At the same time, the WSS obtained from the Carreau Yasuda model was lower than the Newtonian model, thus overestimation of Newtonian model is observed.

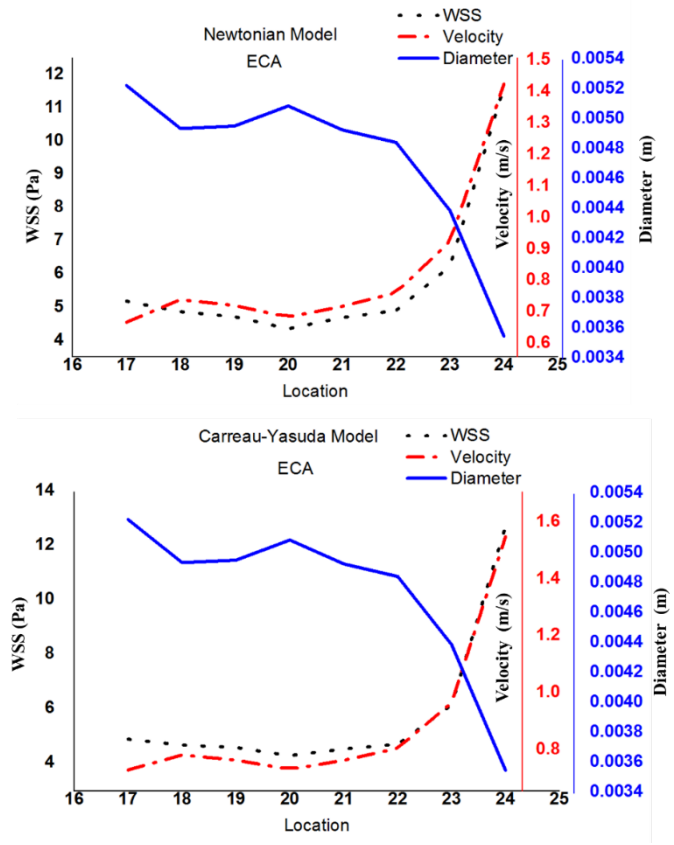

Fig. 13. Variation of WSS, velocity and diameter along the axis of ICA.

4. Conclusions

In the present study, haemodynamics of Newtonian and non-Newtonian models are compared. It is also observed that the shear thinning properties of the blood has less influence on the large arteries as compared with the previous studies. However, even in large arteries, at the region where there is low WSS leading to flow reversals and the region where the diameter is small due to stenosis, the Newtonian model over exaggerates the haemodynamic parameters and less accurately predicts the outcome. It is also observed in the previous studies, that the plaque deposits are located at the carotid sinus region due to sudden enlargement of the lumen area and resulting in recirculation zones. However, in the present study entire ICA is partially stenosed. Hence, it is the clearly indicating that the plaque deposit is not only dependent on the changes in the lumen diameter and the flow recirculation region, but also on the other haemodynamic parameters and blood rheology. Also, the Carreau Yasuda model adopted in present study to evaluate the non-Newtonian properties of blood provides the better approximations at critical locations than Newtonian property. However, in the present study, the effect of arterial wall on the blood flow is not incorporated to understand its influence on the haemodynamics. Present investigation can be useful as fundamental study to compare the haemodynamics in Newtonian and non-Newtonian models related to subject specific cases.

Nomenclatures

a	Yasuda exponent (2)
f	External or Body force
k	Flow consistency index
n	Power law index (0.3568)

Greek Symbols

λ	Relaxation time (3.313 s)
μ_0	Viscosity at zero shear rate (0.056 Pa.s)
μ_∞	Viscosity at is the infinite shear rate (0.0035 Pa.s)
ρ	Constant flow density (1050 kg/m3)
τ	Shear stress tensor
v	Velocity vector

Abbreviations

CCA	Common Carotid Artery
CT	Computed Tomography
ECA	ECA External Carotid Artery
ICA	Internal Carotid Artery
WSS	Wall Shear Stress

References

1. Flaherty, M.L; Kissela, B.; Khoury, J.C.; Alwell, K.; Moomaw, C.J.; Woo, D.; Khatri, P.; Ferioli, S.; Adeoye, O.; Broderick, J.P.; and Kleindorfer, D. (2013). Carotid artery stenosis as a cause of a stroke. *Neuroepidemiology*, 40(1), 36-41.
2. Liepsch, D.; Balasso, A.; Berger, H.; and Eckstein, H.H. (2012). How local haemodynamics at the carotid bifurcation influence the development of carotid plaques. *Perspectives on Medicine*, 1-12(1), 132-136.

3. Malek, A.M.; Alper, S.L. and Izumo, S. (1999). Haemodynamic shear stress and its role in atherosclerosis. *The Journal of the American Medical Association,* 282(21), 2035-2042.
4. Cecchi, E.; Giglioli, C.; Valente, S.; Lazzeri, C.; Gensini, G.F.; Abbate, R.; and Mannini, L. (2011). Role of haemodynamic shear stress in cardiovascular disease. *Atherosclerosis*, 214(2), 249-256.
5. VanderLaan, P.A.; Reardon, C.A.; and Getz, G.S. (2004). Site specificity of Atherosclerosis: Site-selective responses to Atherosclerotic modulators. *Arteriosclerosis, Thrombosis, and Vascular Biology*, 24(1), 12-22.
6. Slager, C.J.; Wentzel, J.J.; Gijsen, F.J.H.; Thury, A.; Van Der Wal, A.C.; Schaar, J.A.; and Serruys, P.W. (2005). The role of shear stress in the destabilization of vulnerable plaques and related therapeutic implications. *Nature Clinical Practice Cardiovascular Medicine*, 2(9), 456-464.
7. Shaaban, A.M.; and Duerinckx, A.J. (2000). Wall shear stress and early atherosclerosis: A Review. *American Journal of Roentgenology*, 174(6), 1657-1665.
8. Cibis, M.; Potters, W.V.; Gijsen, F.J.H.; Marquering, H.; Van Bavel, E.; Van Der Steen, A.F.W.; Nederveen, A.J.; and Wentzel, J.J. (2014). Wall shear stress calculations based on 3D cine phase contrast MRI and computational fluid dynamics: A comparison study in healthy carotid. *NMR in Biomedicine*, 27(7), 826-34.
9. Morbiducci, U.; Gallo, D.; Massai, D.; Consolo, F.; Ponzini, R.; Antiga, L.; Bignardi, C.; Deriu, M.A.; and Redaelli, A. (2010). Outflow conditions for image-based hemodynamic models of the carotid bifurcation: implications for indicators of abnormal flow. *Journal of Biomedical Engineering*, 132(9), 91005.
10. Fan, Y.; Jiang, W.; Zou, Y.; Li, J.; Chen, J.; and Deng, X. (2009). Numerical simulation of pulsatile non-Newtonian flow in the carotid artery bifurcation. *Acta Metallurgica Sinica,* 25(2), 249-255.
11. Gijsen, F.J.; Van De Vosse, F.N.; and Janssen, J.D. (1999). The influence of the non-Newtonian properties of blood on the flow in large arteries: steady flow in a carotid bifurcation model. *Journal of Biomechanics*, 32(6), 601-608.
12. Chen, J.; and Lu, X.Y. (2004). Numerical investigation of the non-Newtonian blood flow in a bifurcation model with a non-planar branch. *Journal of Biomechanics*, 37(12), 1899-1911.
13. Ladak, H.M.; Milner, J.S.; and Steinman, D.A. (2000). Rapid three-dimensional segmentations of the Carotid Bifurcation from serial MR images. *Journal of Biomechanics*, 122(10), 1814-1817.
14. Steinman, D.A.; Poepping, T.L.; Tambasco, M.; Rankin, R.N.; and Holdsworth, D.W. (2000). Flow patterns at the stenosed carotid bifurcation: Effect of concentric versus eccentric stenosis. *Annals of Biomedical Engineering*, 28(4), 415-423.
15. Long, Q.; Xu, X.Y.; Ramnarine, K.V.; and Hoskins, P. (2001). Numerical investigation of physiologically realistic pulsatile flow through arterial stenosis. *Journal of Biomechanics*, 34(10), 1229-1242.
16. Stroud, J.S.; Berger, S.; and Saloner, D. (2002). Numerical analysis of flow through a severely stenotic carotid artery bifurcation. *Journal of Biomechanics*, 124(1), 9-20.

17. Marshall, I.; Zhao, S.; Papathanasopoulou, P.; Hoskins, P.; and Xu, X.Y. (2004). MRI and CFD studies of pulsatile flow in healthy and stenosed carotid bifurcation models. *Journal of Biomechanics*, 37(5), 679-687.
18. Zhao, S.Z.; Papathanasopoulou, P.; Long, Q.; Marshall, I.; and Xu, X.Y. (2003). Comparative study of magnetic resonance imaging and image-based computational fluid dynamics for quantification of pulsatile flow in a carotid bifurcation phantom. *Annals of Biomedical Engineering*, 31(8), 962-971.
19. Li, G.; Chen, B.; and Zhou, G. (2013). Unsteady non-Newtonian solver on unstructured grid for the simulation of blood flow. *Advances in Mechanical Engineering*, 5, 596172.
20. Zarins, C.K.; Giddens, D.P.; Bharadvaj, B.K.; Sottiurai, V.S.; Mabon, R.F.; and Glagov, S.K. (1983). Carotid Bifurcation Atherosclerosis: Quantative correlation of plaque localization with flow velocity profiles and wall shear stress. *Circulation Research*, 53(4), 502-514.
21. Van de Vosse, B.F.N.; and Hart, J. (2003). Finite-element-based computational methods for cardiovascular fluid-structure interaction. *Journal of Engineering Mathematics*, 47, 335-368.
22. Milner, J.S.; Moore, J.; Rutt, B.K.; and Steinman, D. (1998). Haemodynamics of human carotid artery bifurcations: Computational studies with models reconstructed from magnetic resonance imaging of normal subjects. *Journal of Vascular Surgery*, 28(1), 143-156.
23. Taylor, C.A.; Hughes, T.J.R.; and Zarins, C.K. (1998). Finite element modeling of blood flow in arteries. *Computer Methods in Applied Mechanics and Engineering*, 158 (1-2),155-196.
24. Frolov, S.V.; and Sindeev, S.V. (2018). Newtonian and non-Newtonian blood flow at a 90^0 bifurcation of the cerebral artery: A comparative study of fluid viscosity models. *Journal of Mechanics in Medicine and Biology*, 18 (5).
25. Deplano, V.; and Siouffi, M. (1999). Experimental and numerical study of pulsatile flows through stenosis. *Journal of Biomechanics*, 32(10), 1081-1090.
26. Chan, W.Y.; Ding, Y.; and Tu, J.Y. (2007). Modeling of non-Newtonian blood flow through a stenosed artery incorporating fluid-structure interaction. *ANZIAM Journal*, 47; C507-C523.
27. Carlos, O.; Armando, A.S.; André, S.; Sílvia, G.; and Abel, R. (2017). Numerical study of non-Newtonian blood behavior in the abdominal Aortic Bifurcation of a patient-specific at rest. *The Open Sports Sciences Journal*, 10(2-M9), 279-285.
28. Kabinejadian, F.; and Ghista, D.N. (2012). Compliant model of a coupled sequential coronary arterial bypass graft: Effects of vessel wall elasticity and non-Newtonian rheology on blood flow regime and hemodynamic parameters distribution. *Medical Engineering and Physics*, 34, 860-872.
29. Hundertmark, Z.A.; and Lukacova, M.M. (2010). Numerical study of shear dependent non-Newtonian fluids in compliant vessels. *Computers and Mathematics with Applications*, 60:572-590.
30. Gijsen, J.; Allanic, E.; Van de Vosse F.N.; and Janssen, J.D. (1999). The influence of the non-Newtonian properties of blood on the flow in large arteries: unsteady flow in a 90 degrees curved tube. *Journal of Biomechanics*, 32(7), 705-713.

31. Khairuzzaman, M.; Nasrin, A.; and Ken-Ichi, F. (2018). Simulation of physiological Non-Newtonian blood flow through 3-D geometry of carotid artery with Stenosis. *IOSR Journal of Mechanical and Civil Engineering (IOSR-JMCE)*, 15(1), 33-43.
32. Shibeshi S.S.; and Collins. W.E. (2005). The rheology of blood flow in a branched arterial system. *Applied Rheology*, 15(6), 398-405.
33. Johnston, B.M.; Johnston, P.R.; Corney, S.; and Kilpatrick, D. (2004). Non-Newtonian blood flow in human right coronary arteries: Steady state simulations. *Journal of Biomechanics*, May: 37(5), 709-720.
34. Gharahi, B.A.; Zambrano, D. C.; Zhu, J.K.; and Baek. S.; (2016). Computational fluid dynamic simulation of human carotid artery bifurcation based on anatomy and volumetric blood flow rate measured with magnetic resonance imaging. *International Journal of Advances in Engineering Sciences and Applied Mathematics*, 8(1), 46-60.
35. Cho, Y.I.; and Kensey, K.R. (1991). Effects of the non-Newtonian viscosity of blood on flows in a diseased arterial vessel. Part 1: Steady flows. *Biorheology*, 28(3-4), 241-62.
36. Olufsen, M.S. (1999). Structured tree outflow condition for blood flow in larger systemic arteries. *American Journal of Physiology*, 276(1), H257-68.
37. Khader, S.M.; Ayachit, A.; Pai, R.; Muraleedharan, C.V.; Zubair, M.; and Rao, V.R.K. (2016). Experimental and numerical study of Stenotic flows. *Journal of Medical Imaging and Health Informatics*, 6(6), 1500-1506.
38. Ku, D.N. (1997). Blood flow in arteries. *Annual Review of Fluid Mechanics*, 29(1), 399-434.
39. Javadi, M.A.; Ostadhossein, R.; Ghasemiasl, R.; and Hoseinzadeh. (2018). Blood flow simulation in an Aorta with a mild coarctation using magnetic resonance angiography and finite volume method. *International Journal of Engineering*, 31(4), 673-678.
40. Kumar, N.; Khader, A.; Pai, R.; Kyriacou, P.A.; Khan, S.; and Koteshwara, P. (2019). Computational fluid dynamic study on effect of Carreau-Yasuda and Newtonian blood viscosity models on hemodynamic parameters. *Journal of Computational Methods in Sciences and Engineering*, 19(2), 465-477.
41. Olufsen, M.S.; Peskin, C.S.; Kim, W.Y.; Pedersen, E.M.; Nadim, A.; and Larsen, J. (2000). Numerical simulation and experimental validation of blood flow in arteries with structured-tree outflow conditions. *Annual Review of Biomedical Engineering*, 28(11), 1281-1299.
42. Chandra, S.; and Garci. A. (2014). Impedance-based outflow boundary conditions for human carotid haemodynamics. *Computer Methods in Biomechanics and Biomedical Engineering*, 17(11), 1248-1260.
43. Pai, R.; Khader, S.M.A.; Ayachit, A.; Ahmad, K.A.; Zubair, M.; Rao, V.R.K.; and Kamath, S.G. (2016). Fluid-structure interaction study of stenotic flow in subject specific carotid bifurcation-A case study. *Journal of Medical Imaging and Health Informatics*, 6(6), 1494-1499.
44. Yoshihito, O.; Oshima, M.; Toshinori, I.; Hiroaki, K.; Yajima, Y.; Kenji, M.; and Tohnai, I. (2016). Investigation of blood flow in the external carotid artery and its branches with a new 0D peripheral model. *Biomedical Engineering Online*, 15:16.

45. Steinman, D.A. (2012). Assumptions in modelling of large artery hemodynamics in modelling of Physiological flows, Springer Milan Dordrecht Heidelberg London NewYork, 2012, 10-13.

46. Geogheran, P.; Jermy, M.; and Nobes, D. (2017). A PIV comparison of the flow field and wall shear stress in rigid and compliant models of healthy carotid arteries. *Journal of Mechanics in Medicine and Biology*, 17(3),1750041.

    Xiang, M.; Tremmel, J.; Levy, E.I.; Natarajan, S.K.; and H. Meng. (2011). Newtonian viscosity model could overestimate wall shear stress in intracranial aneurysm domes and underestimate rupture risk. *Journal of Neuro-Interventional Surgery,* 4(5), 351-357.

47. Teng, Z.; and Woodard, P.K. (2010). 3D critical plaque wall stress is a better predictor of carotid plaque rupture sites than flow shear stress: An in-vivo MRI-based 3D FSI study. *Journal of Biomechanical Engineering*, 132(3), 1-9.